Self-consistent interface properties of *d*- and *s*-wave superconductors

A. M. Martin and James F. Annett

University of Bristol, H.H. Wills Physics Laboratory, Royal Fort, Tyndall Ave., Bristol BS8 1TL, United Kingdom
(Received 21 August 1997)

We develop a method to solve the Bogoliubov–de Gennes equation for superconductors self-consistently, using the recursion method. The method allows the pairing interaction to be either local or nonlocal, corresponding to *s*- and *d*-wave superconductivity, respectively. Using this method we examine the properties of various *S-N* and *S-S* interfaces. In particular, we calculate the spatially varying density of states and order parameter for the following geometries: (i) *s*-wave superconductor to normal metal, (ii) *d*-wave superconductor to normal metal, (iii) *d*-wave superconductor to *s*-wave superconductor. We show that the density of states at the interface has a complex structure including the effects of normal surface Friedel oscillations, the spatially varying gap and Andeev states within the gap, and the subtle effects associated with the interplay of the gap and the normal van Hove peaks in the density of states. In the case of bulk *d*-wave superconductors, the surface leads to mixing of different order-parameter symmetries near the interface and substantial local filling in of the gap. [S0163-1829(98)07314-7]

I. INTRODUCTION

Interfaces in superconductors, especially high-temperature superconductors, are of considerable interest for both fundamental physics and for applications. Many experiments have used both single electron tunneling and Josephson effects as probes of the energy gap and order parameter symmetry in the cuprates. For example Wollman *et al.*[1] and Sun *et al.*[2] constructed superconducting quantum interference devices consisting of junctions between YBa$_2$Cu$_3$O$_7$ (YBCO) and Pb, while Tsuei *et al.*[3] constructed superconducting rings consisting of YBCO thin films with two or three grain-boundary junctions. Theoretical analysis of experiments such as these relies to a large extent on macroscopic symmetry arguments and not on the microscopic details of the actual interfaces. However, in some cases the microscopic physics at the interface can be an important factor in understanding the experimental results. For example, if mixing of different order-parameter symmetries occurs at the interface (because the interface breaks the bulk tetragonal or orthorhombic symmetry) the extent of such mixing can only be determined from microscopic calculations. Similarly, suppression of the order parameter (either *d*-wave or *s*-wave) near an *S-N* interface can lead to significant local density of states within the bulk energy gap, and this can complicate the analysis of single electron tunneling spectra.[4]. The microscopic physics of surfaces and interfaces of high-T_c superconductors are especially interesting because of the short coherence length, and the probable *d*-wave gap function.

In the past few years there have been a number of microscopic calculations of surfaces and interfaces in superconducting systems with a *d*-wave order parameter. Most of the theoretical results have been obtained using tunneling theory, or Andreev's approximation[5–14] in which the tunneling barrier and the order parameter are not found self-consistently. For tunnel junctions these approximations may be adequate, but we show below that self-consistency has significant effects for interfaces with direct contact between the constituents. Self-consistent properties of interfaces have previously been computed using the Eilenberger equations,[15–20] which are an approximation to the Bogoliubov–de Gennes equation. These self-consistent solutions to the Eilenberger equations have shown some interesting effects that have only arisen when the order parameter is calculated in a self-consistent manner.

In this paper we aim to show how to calculate self-consistent properties of superconducting interfaces by directly solving the Bogoliubov–de Gennes equations. This approach has the advantage that self-consistency can be fully incorporated and also there is no need for the further approximations of the Eilenberger method. Our approach makes use of the recursion method[21] to solve the Bogoliubov–de Gennes equation on an arbitrary tight-binding lattice. Previously, the recursion method has been used to examine the effects of disorder in *s*-wave[22,23] and *d*-wave[24] superconductors, and to determine the core structure of vortices and explain the origin of de Haas–van Alphen oscillations in the superconducting state.[25] In particular, Litak, Miller, and Györffy[23] have given a detailed description of the application of the recursion method to local interactions, corresponding to *s*-wave superconductors. Here we extend this to the case of nonlocal interactions necessary to obtain *d*-wave superconductivity and apply the method to various interfaces of *s* and *d*-wave superconductors. Previous fully self-consistent calculations of the Bogoliubov–de Gennes equation, with nonlocal interactions, have been performed for very small systems, to examine the effect of single impurity scattering[26] and the effect of roughness at superconducting interfaces.[27]

The method of performing our self-consistent calculations will be described in Sec. II. Here we introduce the Bogoliubov–de Gennes equation with a general interaction U_{ij}, and demonstrate how this general Hamiltonian can be solved self-consistently using the recursion method.[21,23] A necessary and nontrivial step in the calculation, as described below, involves finding the density of states accurately by extrapolation of the recursion method continued fraction.

In Sec. III we proceed to apply the method to several different problems. First, various test calculations are de-

scribed, including the local density of states for a uniform system with no interactions, the local density of states for a system with a local attractive interaction (local s-wave superconducting order parameter), and a system with a nonlocal attractive interaction. We show that for this nonlocal interaction there are two possible solutions, these solutions being a nonlocal s-wave superconducting order parameter (extended s-wave) and a nonlocal d-wave superconducting order parameter.

Having tested the method on uniform systems we present our self-consistent solutions for the interface between two different materials. We will consider three different interfaces. First, we consider a normal metal to s-wave superconductor N-S^s interface where the pairing interaction is zero in the normal region (N) and purely local in the superconducting region (S^s). Then we will consider a d-wave to normal metal S^d-N, interface where again the interaction in the normal region is zero and there is a nonlocal attractive interaction in the superconducting region (S^d). Finally, a study of a S^d-S^s interface will be described. These three calculations enable us to make a comparative study of how the local density of states and the order parameter changes as a function of position across the different types of interface.

II. THEORY/MODEL

A. The Bogoliubov–de Gennes equation

The Bogoliubov–de Gennes equation on a tight-binding square lattice has the form

$$\sum_j \mathbf{H}_{ij} \begin{pmatrix} u_j^n \\ v_j^n \end{pmatrix} = E_n \begin{pmatrix} u_i^n \\ v_i^n \end{pmatrix}, \tag{1}$$

with

$$\mathbf{H}_{ij} = \begin{pmatrix} H_{ij} & \Delta_{ij} \\ \Delta_{ij}^\star & -H_{ij}^\star \end{pmatrix}, \tag{2}$$

where u_i^n and v_i^n are the particle and hole amplitudes, on site i, associated with an eigenenergy E_n and where Δ_{ij} is the (possibly nonlocal) pairing potential or gap function.

In the fully self-consistent Bogoliubov–de Gennes equation the normal-state Hamiltonian H_{ij} is given by

$$H_{ij} = (t_{ij} + \tfrac{1}{2} U_{ij} n_{ij})(1 - \delta_{ij})$$
$$+ (\epsilon_i - \mu + \tfrac{1}{2} U_{ii} n_{ii}) \delta_{ij}, \tag{3}$$

where μ is the chemical potential, ϵ_i is the normal on-site energy of site i, and t_{ij} is the hopping integral between site i and site j. For the rest of this paper, t_{ij} is nonzero for nearest neighbors only. The on-site and off-site interaction terms $1/2 U_{ii} n_{ii}$ and $1/2 U_{ij} n_{ij}$ are the Hartree-Fock potentials corresponding to the on-site interaction U_i and the nonlocal interaction U_{ij}. The charge density entering the Hartree-Fock terms n_{ij} is given by

$$n_{ij} = \sum_\sigma \langle \Psi_{i\sigma}^\dagger \Psi_{j\sigma} \rangle = 2 \sum_n (u_i^n)^\star u_j^n f(E_n)$$
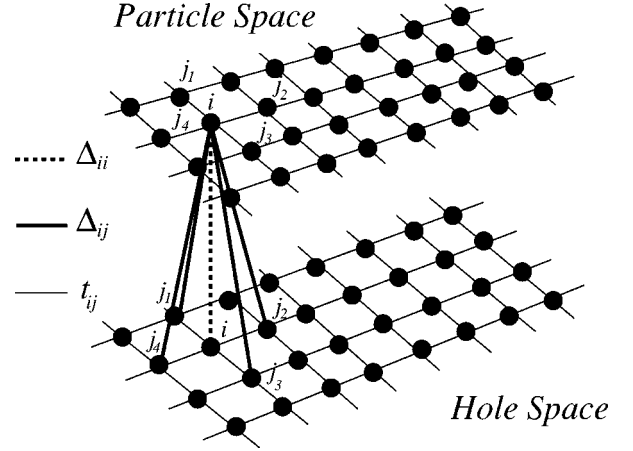$$+ v_i^n (v_j^n)^\star [1 - f(E_n)]. \tag{4}$$

FIG. 1. This is a schematic diagram of a tight-binding lattice, with particle and hole degrees of freedom, Δ_{ij} couples particles on site i to holes on site j. The difference between local and nonlocal pairing is highlighted by the dashed (local pairing) and solid (nonlocal pairing) lines.

Similarly the pairing potentials are defined as

$$\Delta_{ij} = -U_{ij} F_{ij} \tag{5}$$

where the anomalous density is

$$F_{ij} = \langle \Psi_{i\uparrow} \Psi_{j\downarrow} \rangle = \sum_n u_i^n (v_j^n)^\star [1 - f(E_n)]$$
$$- (v_i^n)^\star (u_j^n) f(E_n). \tag{6}$$

In Eqs. (4) and (6) the sums only consider terms E_n up to the condensate chemical potential (μ).

A solution to the above system of equations will be fully self-consistent provided that both the normal ($U_{ij} n_{ij}$) and anomalous (Δ_{ij}) potentials are determined consistently with the corresponding densities n_{ij} and F_{ij} via Eqs. (3) and (5). Note that the normal Hartree-Fock terms $U_{ij} n_{ij}$ play an important role and cannot be neglected. For on-site interactions these terms correspond to position dependent shifts in the on-site energy, while for nonlocal interactions these terms renormalize the hopping t_{ij}, leading to position-dependent changes in the electronic bandwidth.

Figure 1 illustrates the geometry corresponding to this system of equations. The tight-binding lattice has nearest-neighbor hopping interactions (t_{ij}), as well as a coupling between particle and hole space, via a superconducting order parameter (Δ_{ij}). If the interactions are purely on-site (U_{ii}) attractions then the pairing potential will be purely local (Δ_{ii}), corresponding to the dashed line in Fig. 1. On the other hand, when the interaction is nonlocal (U_{ij}, $i \neq j$) the pairing potential Δ_{ij} will also be nonlocal, as illustrated by the solid lines in Fig. 1. For computational convenience we limit both the hopping and nonlocal interaction to nearest-neighbor distances. We also need to specify over what energy range the interaction has an effect, and as in BCS,[28] we will assume that it only acts over a small energy range centered on the Fermi energy, $\mu \pm E_c$.

B. The recursion method

The method we have adopted to solve the above system of equations is the recursion method.[21] This method allows us to calculate the electronic Green's functions

$$G_{\alpha\alpha'}(i,j,E) = \langle i\alpha | \frac{1}{E\mathbf{1}-H} | j\alpha' \rangle, \qquad (7)$$

where the indices i and j denote sites, while α and α' represent the particle or hole degree of freedom on each site. We

denote particle degrees of freedom by $\alpha = +$ and hole degrees of freedom by $\alpha = -$. For example $G_{+-}(i,j,E)$ represents the Green's function between the particle degree of freedom on site i and the hole degree of freedom on site j.

To compute the Green's functions (7), we can closely follow the method described by Litak, Miller, and Györffy[23] for the special case of a local interaction ($U_{ij} = U_i \delta_{ij}$). Using their method we can transform the Hamiltonian to a block tridiagonal form

$$E\mathbf{1}-H = \begin{pmatrix} E\mathbf{1}-a_0 & -b_1 & 0 & 0 & 0 & 0 & 0 & \cdots \\ -b_1^\dagger & E\mathbf{1}-a_1 & -b_2 & 0 & 0 & 0 & 0 & \cdots \\ 0 & -b_2^\dagger & \ddots & \ddots & 0 & 0 & 0 & \cdots \\ 0 & 0 & \ddots & \ddots & \ddots & 0 & 0 & \cdots \\ 0 & 0 & 0 & -b_n^\dagger & E\mathbf{1}-a_n & -b_{n+1} & 0 & \cdots \\ \vdots & \vdots & \vdots & 0 & \ddots & \ddots & \ddots & \ddots \end{pmatrix}, \qquad (8)$$

where a_n and b_n are 2×2 matrices. Given this form for $\langle i\alpha | E\mathbf{1}-H | j\alpha' \rangle$ and expressing the Green's function as

$$G_{\alpha\alpha'}(i,j,E) = \langle i\alpha | (E\mathbf{1}-H)^{-1} | j\alpha' \rangle, \qquad (9)$$

the Green's functions above can be evaluated as a matrix continued fraction so that

$$G(i,j,E) = (E\mathbf{1}-a_0-b_1^\dagger\{E\mathbf{1}-a_1-b_2^\dagger[E\mathbf{1}-a_2-b_3^\dagger$$
$$\times (E\mathbf{1}-a_3-\ldots)^{-1}b_3]^{-1}b_2\}^{-1}b_1)^{-1}, \qquad (10)$$

where

$$G(i,j,E) = \begin{pmatrix} G_{\alpha\alpha}(i,i,E) & G_{\alpha\alpha'}(i,j,E) \\ G_{\alpha'\alpha}(j,i,E) & G_{\alpha'\alpha'}(j,j,E) \end{pmatrix}. \qquad (11)$$

Within Eqs. (8) and (10) we have a formally exact representation of the Green's functions. However in general both the tridiagonal representation of the Hamiltonian, and the matrix continued fraction (8) will be infinite. In practice one can only calculate a finite number of terms in the continued fraction exactly. In the terminology of the recursion method it is necessary to *terminate* the continued fraction.[21,23,29–33]

If we were to calculate up to and including a_n and b_n and then simply set subsequent coefficients to zero, then the Green's function would have $2n$ poles along the real axis. The density of states would then correspond to a set of $2n$ δ functions. Integrated quantities such as the densities n_{ij} and F_{ij} could depend strongly on n, especially since only a few of the $2n$ δ functions would be within the relevant energy range within the BCS cutoff, E_c. In order to obtain accurate results it would be necessary to calculate a large number of exact levels, which would be expensive in terms of both computer time and memory.

As a more efficient alternative we choose to terminate the continued fraction using the extrapolation method, as used

previously by Litak, Miller, and Györffy.[23] We calculate the values for a_n and b_n exactly up to the first m coefficients using the recursion method. Then, noting the fact that the elements of the matrices a_n and b_n vary in a predictable manner,[23] we extrapolate the elements of the matrices for a further k iterations, where k is usually very much greater than m. This enables us to compute the various densities of states, and the charge densities n_{ij} and F_{ij} accurately with relatively little computer time and memory.

In terms of the Green's functions $G_{\alpha\alpha'}(i,j,E)$, the pairing and normal Hartree-Fock potentials Δ_{ij} and $1/2 U_{ij} n_{ij}$ are given by

$$\Delta_{ij} = \frac{1}{2\pi} U_{ij} \int_{-E_c}^{E_c} [G_{+-}(i,j,E+\iota\eta) - G_{+-}(i,j,E-\iota\eta)]$$
$$\times [1-f(E)]dE \qquad (12)$$

and

$$\frac{1}{2} U_{ij} n_{ij} = \frac{1}{2\pi} U_{ij} \int_{-E_c}^{E_c} [G_{++}(i,j,E+\iota\eta)$$
$$- G_{++}(i,j,E-\iota\eta)]f(E)dE, \qquad (13)$$

where η is a small positive number.

To obtain the above equations we have used the fact that

$$\begin{pmatrix} u_i^n \\ v_i^n \end{pmatrix} \quad \text{and} \quad \begin{pmatrix} -(v_i^n)^\star \\ (u_i^n)^\star \end{pmatrix} \qquad (14)$$

are the eigenvectors of Eq. (1) with eigenvalues E_n and $-E_n$ respectively. Also note that the integrals in Eqs. (12) and (13) are bounded by the cutoff E_c, corresponding to the energy dependent interaction

$$U_{ij}(E) = \begin{cases} -|U| & \text{for } |E-\mu| \leq E_c \\ 0 & \text{for } |E-\mu| > E_c, \end{cases} \qquad (15)$$

TABLE I. This table shows which Green's functions need to be calculated for systems with interactions which are local, U_{ii}, nonlocal, $U_{ij}(1-\delta-ij)$, or both. The site labels correspond to the notation of Fig. 1.

Interaction Type	$G_{+-}(i,i,E)$	$G_{+\pm}(i,j_1,E)$	$G_{+\pm}(i,j_2,E)$	$G_{+\pm}(i,j_3,E)$	$G_{+\pm}(i,j_4,E)$
U_{ii}	Y	N	N	N	N
$U_{ij}(1-\delta_{ij})$	N	Y	Y	Y	Y
$U_{ii}+U_{ij}(1-\delta_{ij})$	Y	Y	Y	Y	Y

as in BCS theory. Our cutoff E_c can correspond to the BCS cutoff $\hbar\omega_D$ arising from retardation of the electron-phonon interaction, or any other energy scale cutoff for the interaction that may be applicable for high-temperature superconductors.

C. Achieving self-consistency

Using the above methods to calculate Δ_{ij} and $U_{ij}n_{ij}$ we need to achieve a fully self-consistent solution. First, we make use of any symmetries in the system in order to minimize the number of calculations that are necessary. For example, on an infinite square lattice with no variation in any of the potentials, only one independent site needs to be calculated since this site can be mapped onto all of the other sites. Second, once we have decided which sites need to be calculated self-consistently, Δ_{ij} and n_{ij} can be calculated for those sites, remembering that on a square lattice each site will have four nearest neighbors. This implies that in general we will have to calculate nine different Green's functions in order to calculate Δ_{ij} and n_{ij}. This can be seen by considering site i in Fig. 1 and noting that we need to calculate the Green's functions shown in Table I, depending on whether the interaction is purely local, purely nonlocal, or both local and nonlocal. Having calculated the appropriate Green's functions, new values for Δ_{ij} and n_{ij} can be calculated, which we will denote as $\Delta_{ij}^{(1)}$ and $n_{ij}^{(1)}$. Inserting these into the Hamiltonian and repeating the calculation of the Green's functions leads to a new set $\Delta_{ij}^{(2)}$ and $n_{ij}^{(2)}$ and so on. We repeat this iteration for all i and j until

$$\left|\frac{|\Delta^{(n-1)}|-|\Delta^{(n)}|}{|\Delta^{(n)}|}\right|\leq 0.001 \qquad (16)$$

and

$$\left|\frac{|n^{(n-1)}|-|n^{(n)}|}{|n^{(n)}|}\right|\leq 0.001. \qquad (17)$$

Since Δ_{ij} and n_{ij} can be complex, we need to also check for convergence in their associated phases. We do this and find that convergence in the phase gradient of the complex parameters is much more rapid than the convergence in the magnitude.

III. NUMERICAL RESULTS

A. Uniform systems

As a first test of the above methods let us examine a bulk superconductor, corresponding to an infinite 2D square lattice with either local or nonlocal attraction. These examples will show how well such quantities as the local particle den-

sity of states can be calculated and how the extrapolation of the elements of the matrices a_n and b_n is performed.

The quantity of interest is the local particle density of states, which can be calculated from the following expression:

$$N_i(E)=\frac{1}{2\pi}[G_{++}(i,i,E+\iota\eta)-G_{++}(i,i,E-\iota\eta)]. \qquad (18)$$

Consider first a noninteracting system where $U_{ij}=0$, $\mu=0$, $\epsilon_i=0$, and $t_{ij}=1$ for nearest neighbors and zero everywhere else. Figure 2 shows the local particle density of states for a calculation where the number of exact continued fraction levels was $m=50$ and the elements of a_n and b_n were extrapolated for 2000 more values. For this calculation the convergence parameter η was chosen as $\eta=0.02$. Figure 2 shows that using the extrapolation method the central logarithmic van Hove singularity and the sharp band edges can be resolved very well. Figure 3 shows the first 100 continued fraction coefficients $\mathfrak{R}b_n^{11}$, where the first 50 are calculated directly using the recursion method and the rest are the extrapolated values. It is clear from the figure that the oscillations in $\mathfrak{R}b_n^{11}$ still persist after the first 50 continued fraction levels. In fact, these oscillations die off slowly, as $1/n$, and it is critical to include them correctly. From Fig. 3 it is clear that the first 50 levels provide enough information about the decaying oscillation so that the $\mathfrak{R}b_n^{11}$ can be extrapolated quite easily.

Having considered a system where the interaction is zero, the next step is to consider systems where the interaction is uniform and finite. For such systems the local particle den-
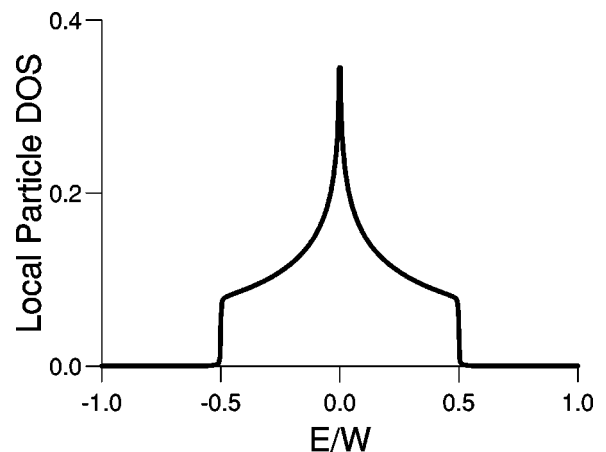

FIG. 2. The local particle density of states for a 2D tight binding lattice with no interactions ($U_{ij}=0$). For this system $t_{ij}=1$ for nearest neighbors only, $\mu=0$ and $\epsilon_i=0$.
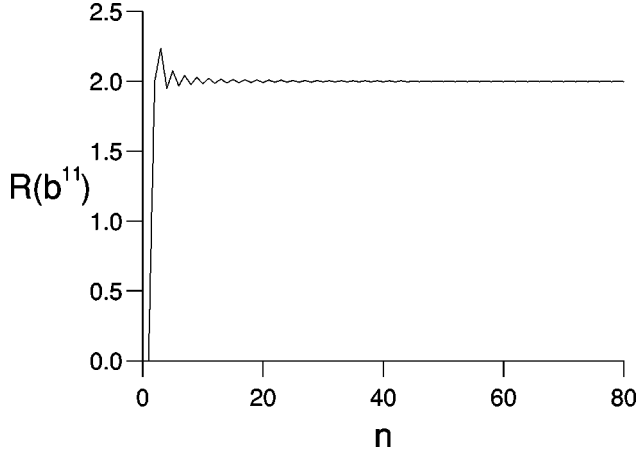
FIG. 3. A plot of the real part of b_n^{11} for the same system that was used to calculate the local particle density of states in Fig. 2.

sity of states can be calculated, for different types of interaction. In Fig. 4 we have plotted two different local particle densities of states for a local interaction $U_{ij} = -2.5\delta_{ij}$ (dashed line) and $U_{ij} = -2.5(1-\delta_{ij})$ for nearest neighbors (solid line). In each case $E_c = 4$ and $t_{ij} = 1$ (for nearest neighbors) and all other parameters were set to zero throughout the lattice.

The dashed line in Fig. 4 clearly shows the energy gap at the Fermi energy, characteristic of s-wave superconductivity. The van Hove peak in the density of states is also very clearly resolved. The solid line in Fig. 4 shows the local particle density of states going to zero at the Fermi energy, in a manner that is typical of the local particle density of states for a d-wave superconductor. In this case of the nonlocal interaction the order parameter changes sign as we rotate by $\pi/2$ around a site, i.e., in reference to Fig. 1 $\Delta_{ij_1} = -\Delta_{ij_2}$, $\Delta_{ij_2} = -\Delta_{ij_3}$ and $\Delta_{ij_4} = -\Delta_{ij_3}$. The way we have performed the calculation is to keep the Fermi energies the same in the two calculations but change, in the case of the local interaction (dashed line), the density and, in the case of the nonlocal interaction (solid line), the width of the band self-consistently. This has the effect of moving the system away
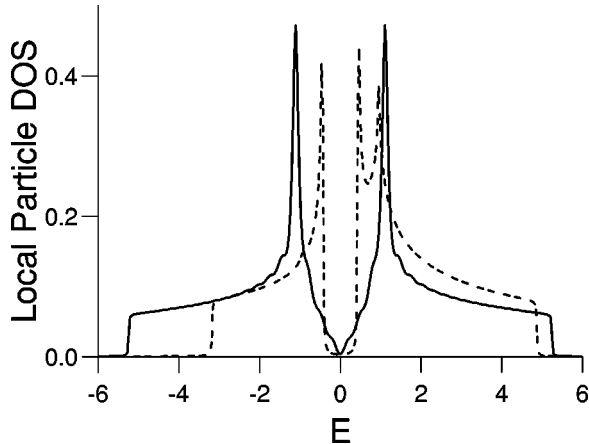

FIG. 4. Two plots of the local particle density of states for, a local interaction [$U_{ij}\delta_{ij} = -2.5$, $U_{ij}(1-\delta_{ij}) = 0$ (dashed line)] and a nonlocal interaction [$U_{ij}\delta_{ij} = 0$, $U_{ij}(1-\delta_{ij}) = -2.5$ (solid line)]. All the other parameters are equal to those used to obtain Fig. 2.

from half filling in the case of the local interaction, and, broadening the band in the case of the nonlocal interaction, because of the local and nonlocal Hartree-Fock terms in the Hamiltonian $U_{ii}n_{ii}$ and $U_{ij}n_{ij}$, respectively.

At this point one should note that in the case of a nonlocal interaction as well as having a d-wave self-consistent solution to the Bogoliubov–de Gennes equation, it is also possible to obtain an extended s-wave solution, i.e., $\Delta_{ij_1} = \Delta_{ij_2}$, $\Delta_{ij_2} = \Delta_{ij_3}$, and $\Delta_{ij_4} = \Delta_{ij_3}$. However we find that such solutions are less stable than the d-wave solutions; this is only true at or near half filling of the band.

To obtain the results shown in Fig. 4 we have again calculated 50 levels of the recursion method exactly and then extrapolated for a further 2000 levels. This can easily be done because the elements of a_n and b_n vary in a predictable manner, as has already been seen for the case without interactions.

B. Interfaces

Having considered systems where the interactions remain uniform throughout the structure the next step is to consider systems that contain interaction strengths which vary in real space. The most simple case one can conceive for this scenario is an interface. We will simply model the interface by allowing the interaction to change in a steplike manner.

We will consider three separate situations, N-S^s, S^d-N, and S^d-S^s. In the normal region we shall set $U_{ij} = 0$, hence the order parameter in this region will be zero, (but one should note that this does not imply that F_{ij} is zero). Before we look at the numerical results it is worthwhile considering what one may expect to find. In the case of a local interaction the results are well documented, i.e., the magnitude of the superconducting order parameter reaches a maximum at the bulk value a few coherence lengths in the superconducting region away from the normal interface. In the case of the nonlocal interaction we would also expect the amplitude of the superconducting order parameter to reach a maximum several coherence lengths away from the interface, but the problem of how to define the magnitude of the superconducting order parameter now arises. Going back to Fig. 1 we can see that for each site i there are five Δ_{ij}'s, so hence for each site we can define five order parameters per site. We can also combine these different order parameters on each site in the following manner:

$$|\Delta_i^{[s(\text{local})]}| = |\Delta_i|, \tag{19}$$

$$|\Delta_i^{(d)}| = \tfrac{1}{4}|\Delta_{ij_1} - \Delta_{ij_2} + \Delta_{ij_3} - \Delta_{ij_4}|, \tag{20}$$

$$|\Delta_i^{[s(\text{nonlocal})]}| = \tfrac{1}{4}|\Delta_{ij_1} + \Delta_{ij_2} + \Delta_{ij_3} + \Delta_{ij_4}|, \tag{21}$$

so that each equation defines a different type of symmetry for that site. Since the systems we are interested in change in the x direction only it is possible, when one is considering the properties of that interface, to look along one line of sites in the x-direction and note that for any other y coordinate the properties of the system are the same, so $\Delta_i \rightarrow \Delta(x)$.

Having defined all the quantities of interest the next step is to specify some of the systems of interest. The three systems we are going to consider are as already pointed out

	$x<100$			$x \geq 100$		
System	U_{ii}	$U_{ij}(1-\delta_{ij})$	E_c	U_{ii}	$U_{ij}(1-\delta_{ij})$	E_c
$N-S^s$	0	0	0	-2.5	0	4.0
S^d-N	0	-3.5	4.0	0	0	0
S^d-S^s	0	-3.5	4.0	-2.5	0	4.0

N-S^s, S^d-N, and S^d-S^s; to set up these systems we used the parameters shown in Table II.

Figures 5(a)–5(c) plot the three main symmetry components of the order parameter $|\Delta^{[s(\text{local})]}(x)|$ (dashed line), $|\Delta^{(d)}(x)|$ (circles) and $|\Delta^{[s(\text{nonlocal})]}(x)|$ (solid line) for the three different geometries $N-S^s$ [Fig. 5(a)], S^d-N [Fig. 5(b)], and S^d-S^s [Fig. 5(c)]. The interface corresponds to $x=100$ on the figures. Figure 5(a) shows, as expected, that the s-wave order parameter, $|\Delta^{[s(\text{local})]}(x)|$, simply rises over a coherence length to a maximum at the bulk superconducting order parameter. Because the interaction is purely on-site in Fig. 5(a) $|\Delta^{(d)}(x)|=|\Delta^{[s(\text{nonlocal})]}(x)|=0$

In Fig. 5(b) we see that for the d-wave to normal metal interface $|\Delta^{(d)}(x)|$ also drops to zero at the interface. However, unlike the s-wave case, it does not simply drop to zero smoothly but has a sharp peak structure right at the interface. The origin of this peak is explained by looking at the extended s-wave component, $|\Delta^{[s(\text{nonlocal})]}(x)|$ [solid line in Fig. 5(b)]. We see that the extended s-wave gap function is

finite near the interface. This is due to the fact that the order parameter varies near the interface and hence $\Delta_{j_1}(x) \neq \Delta_{j_3}(x)$, making the values of $|\Delta^{[s(\text{nonlocal})]}(x)|$. This is emphasized in Fig. 5(d) where $\Delta_{j_3}(x)-\Delta_{j_1}(x)$ is plotted, from this graph one can see that the peak in $|\Delta^{(d)}(x)|$, in Fig. 5(b), near the interface is due to the component in the x direction.

Figure 5(c) shows the d-wave to s-wave superconductor interface. Again we can see that the extended s-wave component $|\Delta^{[s(\text{nonlocal})]}(x)|$ is nonzero at the interface, even though it is zero in the bulk on both sides, and that this leads to sharp features in both the local s-wave and d-wave order parameters near the interface.

Having seen how the profiles of the superconducting order parameters are affected by the proximity of different materials, we now look at how the local particle density of states changes as we move across the various interfaces. Figures 6, 7, and 8 are contour plots of the local particle densities of states for the three interfaces of interest. Figure 6 shows a contour plot for the $N-S^s$ interface. Looking at this plot one can see that as we move across the interface, at $x=100$, the superconducting gap opens up within a couple of atomic sites. On the normal-metal side, for $x<100$, the van Hove singularity in the center of the band can be clearly seen, but as we move into the superconducting region the band edges are shifted (due to the Hartree-Fock potential term) and the superconducting gap opens up at $E=0$. In the superconducting region the van Hove singularity is shifted away from $E=0$, as can also be seen in Fig. 3 (dashed line). Due to the mismatch in the band edges we see oscillations in the local particle density of states near the band edges; these are simply Friedel oscillations.[34,35]
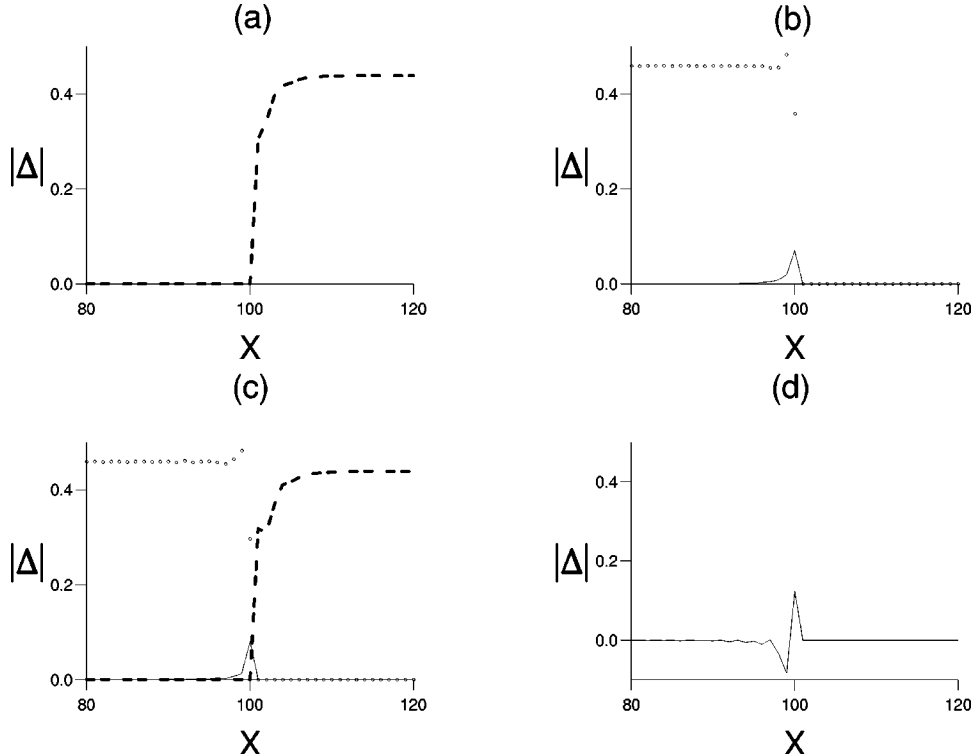

FIG. 5. (a)–(c) plot the profiles of different symmetries of the superconducting order parameter $[|\Delta^{[s(\text{nonlocal})]}(x)|$ (solid line), $|\Delta^{[s(\text{local})]}(x)|$ (dashed line) and $|\Delta^{(d)}(x)|$ (circles)] for different interfaces. (a), (b), and (c) are for N-S^s, S^d-N and S^d-S^s interfaces respectively. 5(d) plots $\Delta_{j_1}(x)-\Delta_{j_3}(x)$ for the N-S^d interface. The parameters used to obtain the figures are given in Table II.
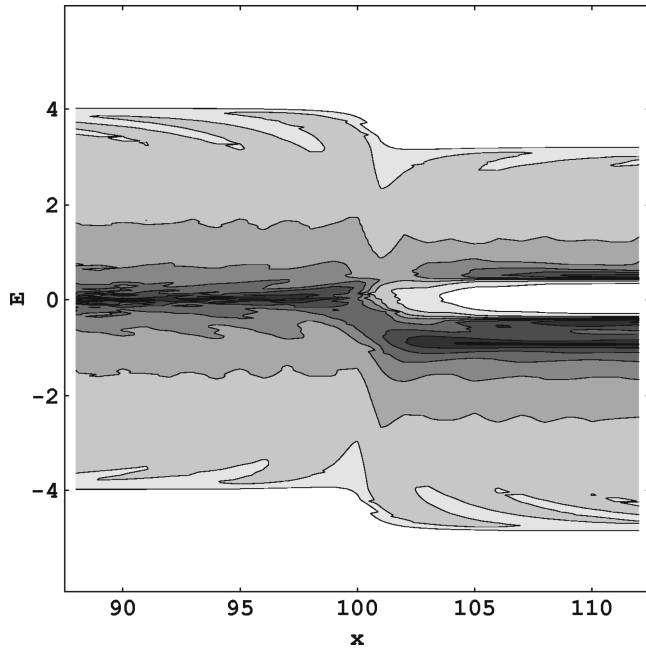
FIG. 6. This is a contour plot of the local particle density of states as a function of position, as one moves across the N-S^s interface. The steps in the contour plot are in units of 0.04, i.e., white represents $N(E) < 0.04$ and black represents $N(E) > 0.32$. The parameters used to obtain this graph are given in Table II.

Figure 7 shows a similar contour plot of the local particle density of states for an S^d-N interface. Again we can clearly see the gap in the superconducting region and the van Hove singularity in the normal region. In this system the Hartree-Fock potential term leads to an increase in overall band width on the d-wave side. Again, since the band edges do not
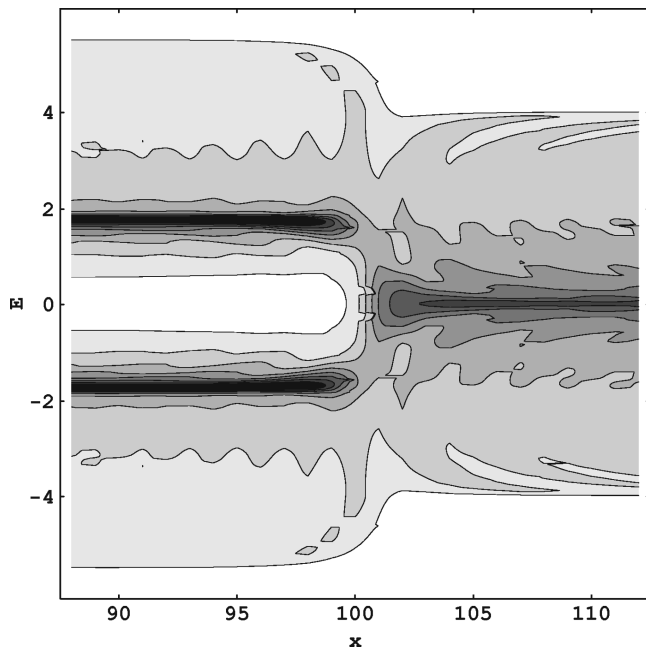

FIG. 7. This is a contour plot of the local particle density of states as a function of position, as one moves across the S^d-N interface. The steps in the contour plot are in units of 0.04, i.e., white represents $N(E) < 0.04$ and black represents $N(E) > 0.32$. The parameters used to obtain this graph are given in Table II.
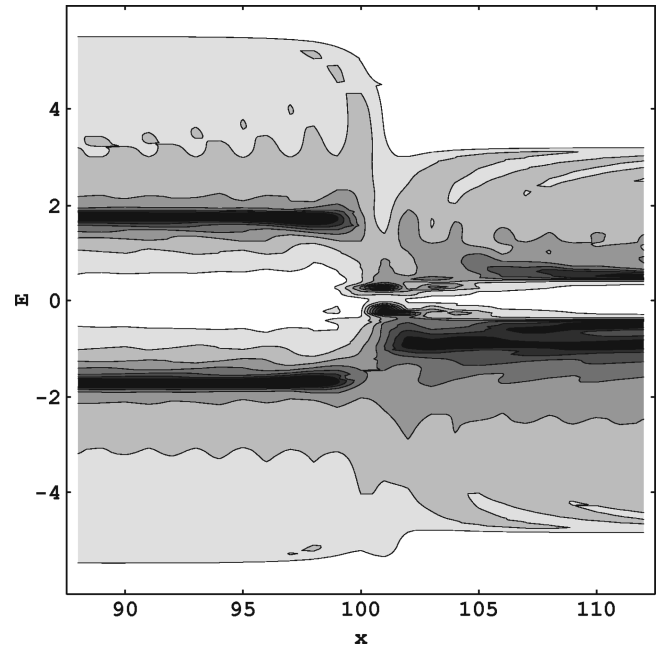

FIG. 8. This is a contour plot of the local particle density of states as a function of position, as one moves across the $S^d - S^s$ interface. The steps in the contour plot are in units of 0.04, i.e., white represents $N(E) < 0.04$ and black represents $N(E) > 0.32$. The parameters used to obtain this graph are given in Table II.

match up, we see Friedel oscillations in the local particle density of states near the band edges.

Finally, in Fig. 8 we have plotted the local particle density of states as we move across the S^d-S^s interface. This plot has many interesting features. The first to note is that, again due to the mismatch in the band edges, oscillations appear in the local particle density of states. Second, for $x < 100$ (S_d region) the density of states gradually goes to zero at $E = 0$ (typical of d-wave superconductivity [see Fig. 4 (solid line)]), whereas for the S^s region the local particle density of states drops to zero very sharply. The main points of interest are what happens at the interface itself. In the plane of the interface there are states in the gap, as both the d-wave and s-wave order parameters are suppressed. At $x = 100$ there are two peaks in the density of states just above and below $E = 0$, which as we move further into the S^s region are shifted to become the BCS density of states singularities just above and below the superconducting gap. Note that the parameters for the calculation in Fig. 8 were chosen so that $|\Delta^{(d)}| \gg |\Delta^{[s(\text{local})]}|$ as would be the case for a YBCO-Pb junction such as those used by Wollman *et al.*[1]

IV. CONCLUSIONS

In this paper we have shown how it is possible to perform self-consistent calculations of the Bogoliubov–de Gennes equation, using the recursion method. This method has the advantage of being an order N method and hence allows us to tackle problems with a relatively small amount of computational effort. A key to obtaining accurate densities of states with relatively little computational effort is the extrapolation procedure we have used to terminate the matrix continued fraction. Our method is fully self-consistent, including both

self-consistency in the order parameter and in the normal Hartree-Fock potentials. As we have shown, these normal potentials make significant contributions by shifting or widening the density of states in a spatially dependent manner. Our method can deal with both local attractive interactions, corresponding to local s-wave superconductivity, or nonlocal interactions corresponding to d-wave or extended s-wave pairing. In our system we found that the d-wave state is more stable.

As a first application of the method, we examined three simple interfaces, corresponding to an s-wave S-N junction, a d-wave S-N junction, and an s-wave to d-wave S-S junction. The numerical results show a number of interesting features, including a non-monotonic variation of the order parameters near the interface, a surface layer of extended s-wave pairing (even though it is not stable in the bulk), and subtle effects of the self-consistent Hartree-Fock terms in the Bogoliubov de Gennes Hamiltonian leading to Friedel oscillations and spatially dependent shifts in the van Hove singu-larities near the interfaces, as highlighted by the contour plot in Fig. 8. We note that at the plane of the interface between the d and s-wave superconducting regions there are states in the gap.

In the future we hope to apply our method to more complex interfacial phenomena in superconductors, such as junctions carrying supercurrent (e.g., to look for π junctions), superconducting twin boundaries, and grain-boundary junctions. Our methods can also be applied to many other problems in superconductivity, such as the structure of vortex cores in s- or d-wave superconductors, the effects of impurities, and so on.

[1] D. A. Wollman, D. J. van Harlingen, W. C. Lee, D. M. Ginsberg, and A. J. Leggett, Phys. Rev. Lett. **71**, 2134 (1993).

[2] A. G. Sun, D. A. Gajewski, M. B. Maple, and R. C. Dynes, Phys. Rev. Lett. **72**, 2267 (1994).

[3] C. C. Tsuei *et al.*, Phys. Rev. Lett. **73**, 593 (1994).

[4] K. Kitizawa, Science **271**, 313 (1996).

[5] C. R. Hu, Phys. Rev. Lett. **72**, 1526 (1994).

[6] J. H. Xu, J. H. Miller, and C. S. Ting, Phys. Rev. B **53**, 3604 (1996).

[7] Y. Tanaka and S. Kashiwaya, Phys. Rev. Lett. **74**, 3451 (1995).

[8] J. X. Zhu, Z. D. Wang, and H. X. Tang, Phys. Rev. B **54**, 7354 (1996).

[9] Y. Tanaka, Phys. Rev. Lett. **72**, 3871 (1994).

[10] S. Kashiwaya, Y. Tanaka, M. Koyanagi, H. Takashima, and K. Kajimura, Phys. Rev. B **51**, 1350 (1994).

[11] H. X. Tang, Z. D. Wang, and J. X. Zhu, Phys. Rev. B **54**, 12 509 (1996).

[12] M. Suzuki, M. Taira, and X. Zheng, Czech. J. Phys. **46**, 1351 (1996).

[13] Y Tanaka and S. Kashiwaya, Phys. Rev. B **56**, 892 (1997).

[14] L. Alff, H. Takashima, S. Kashiwaya, N. Terada, H. Ihara, Y. Tanaka, M. Koyanagi, and K. Kajimura, Phys. Rev. B **55**, R14 757 (1997).

[15] Y. S. Barash, A. V. Galaktionov, and A. D. Zaikin, Phys. Rev. B **52**, 665 (1995).

[16] M. Matsumoto and H. Shiba, J. Phys. Soc. Jpn. **64**, 3384 (1995).

[17] M. Matsumoto and H. Shiba, J. Phys. Soc. Jpn. **64**, 4867 (1995).

[18] M. Matsumoto and H. Shiba, J. Phys. Soc. Jpn. **65**, 2194 (1996).

[19] Y. S. Barash, A. A. Svidzinsky, and H. Burkhardt, Phys. Rev. B **55**, 15 282 (1997).

[20] Y. Morita, M. Kohmoto, and K. Maki, Phys. Rev. Lett. **78**, 4841 (1997).

[21] R. Haydock, in *Solid State Physics*, edited by D. Ehrenreich, F. Seitz, and D. Turnbull (Academic, New York, 1980), Vol. 35.

[22] J. F. Annett and N. D. Goldenfeld, J. Low Temp. Phys. **89**, 197 (1992).

[23] G. Litak, P. Miller, and B. L. Györffy, Physica C **251**, 263 (1995).

[24] T. Xiang and J. M. Wheatley, Phys. Rev. B **51**, 11 721 (1995).

[25] P. Miller and B. L. Györffy, J. Phys.: Condens. Matter **7**, 5579 (1995).

[26] Y. Onishi, Y. Ohashi, Y. Shingaki, and K. Miyake, J. Phys. Soc. Jpn. **65**, 675 (1995).

[27] Y. Tanuma, Y. Tanaka, M. Yamashiro, and S. Kashiwaya, Physica C **282-287**, 1857 (1997).

[28] J. Bardeen, L. N. Cooper, and J. R. Schieffer, Phys. Rev. **108**, 1175 (1957).

[29] A. Magnus, in *Solid State Sciences 58,* edited by D. G. Pettifor and D. L. Weaire (Springer-Verlag, Berlin, 1985).

[30] F. Ducastelle, P. Turchi, and G. Tréglia, in Ref. 29.

[31] C. M. M. Nex, in Ref. 29.

[32] G. Allan, in Ref. 29.

[33] A. Trias, M. Kiwi, and M. Weissmann, Phys. Rev. B **28**, 1859 (1983).

[34] O. Entin-Wohlman and J. Bar-Sagi, Phys. Rev. B **18**, 3174 (1977).

[35] Y. Tanaka and M. Tsukada, Phys. Rev. B **42**, 2066 (1990).

Author/s:
Martin, AM; Annett, JF

Title:
Self-consistent interface properties of d- and s-wave superconductors

Date:
1998-04-01

Persistent Link:
http://hdl.handle.net/11343/43083